Electronic Supporting Information:

How to predict the location of the defect levels induced by 3d transition metal ions in octahedral sites of aluminate phosphors

Bingyan Qu[a], Rulong Zhou[a], Lei Wang*[a, b] and Pieter Dorenbos*[b]

a School of Materials Science and Engineering, Hefei University of Technology, Hefei, Anhui 230009, P. R. China

b Faculty of Applied Sciences, Delft University of Technology, Mekelweg 15, 2629 JB Delft, The Netherlands

*Corresponding author: Lei Wang leiwang@hfut.edu.cn and Pieter Dorenbos p.dorenbos@tudelft.nl.

A. The electronic structure of α-Al_2O_3 and YAG

Fig.S1(a) shows the band structure, total and partial density of states of α-Al_2O_3, from which a large band gap of about 6.18 eV is found. This gap is about 3.32 eV smaller than that of the experimental value (9.5 eV) [1], due to the well-known limitations of GGA-PBE in reproducing the band gaps of semiconductors or insulators. The partial density of states tell us that the higher valence bands distribute in an energy range of about 7 eV, which are mostly contributed by O 2p states. The conduction bands come from O 2p, Al 3s and 3p states.

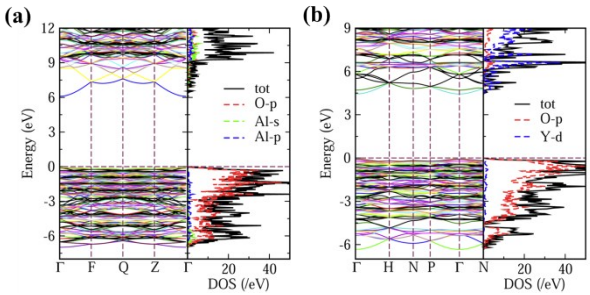

Figure S1 (colour online) Computed band structure, total and projected density of states (DOS and PDOS) of (a) α-Al_2O_3 and (b) YAG. The Fermi level is set to 0 eV.

For YAG, the electronic structure is exhibited in Fig. S1(b). The calculated band gap is about 4.52 eV, whereas the experimental value is 7.67 eV[2]. The band gap of YAG is

smaller than that of α-Al_2O_3. The top of the valence bands are mostly contributed by O 2p states, which is similar with those of α-Al_2O_3. For the conduction bands, besides O 2p states, Y 4d states also have large contribution.

B. The electronic structure of different valence states of M in α-Al_2O_3

The electronic structures of both initial and final states in the calculation of OTL of M ions in α-Al_2O_3 are shown from Fig.S2 to Fig.S11. To obtain M ions in different charge states, we add some electrons to the system or take some electrons from the system. In these calculations, we should notice that the electron added to the system should occupy the 3d orbitals or the electron taken out from the system should come from the 3d orbitals. Based on this consideration, the Sc^{4+} has not considered in our calculations since Sc atom only has three valence electron and so only Sc^{3+} and Sc^{2+} have been computed (Fig.S2).

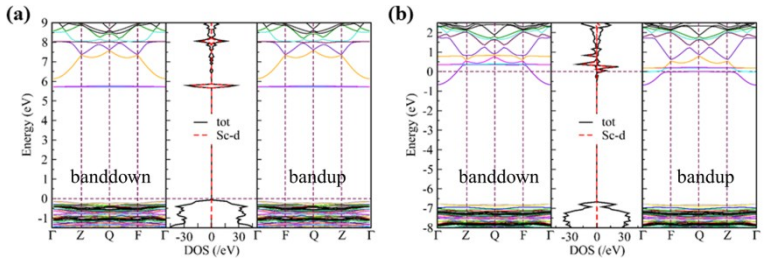

Figure S2 (colour online) The electronic structures of Al_2O_3:Sc in the calculations of OTL $\varepsilon_f(Sc^{n+/(n-1)+})$. (a) is the initial states with n = 3, and (b) is the final states with n = 3. The Fermi level is set to 0 eV.

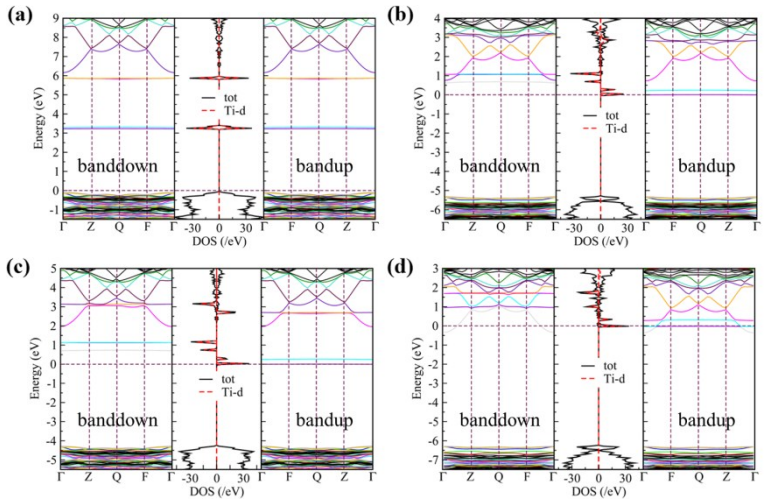

Figure S3 (colour online) The electronic structures of Al_2O_3:Ti in the calculations of OTL $\varepsilon_f(Ti^{n+/(n-1)+})$. (a) and (c) are the initial states with n = 4 and 3, while (b) and (d) are the final state with n = 4 and 3. The Fermi level is set to 0 eV.

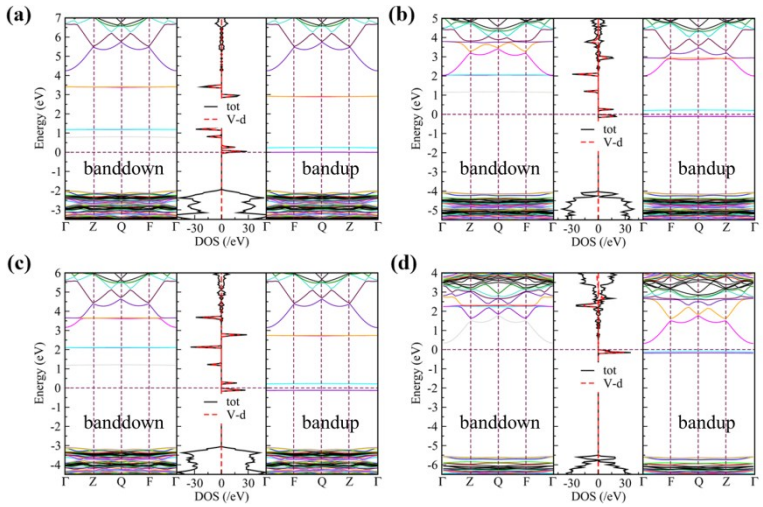

Figure S4 (colour online) The electronic structures of Al_2O_3:V in the calculations of OTL $\varepsilon_f(V^{n+/(n-1)+})$. (a) and (c) are the initial states with n = 4 and 3, while (b) and (d) are the final state with n = 4 and 3. The Fermi level is set to 0 eV.

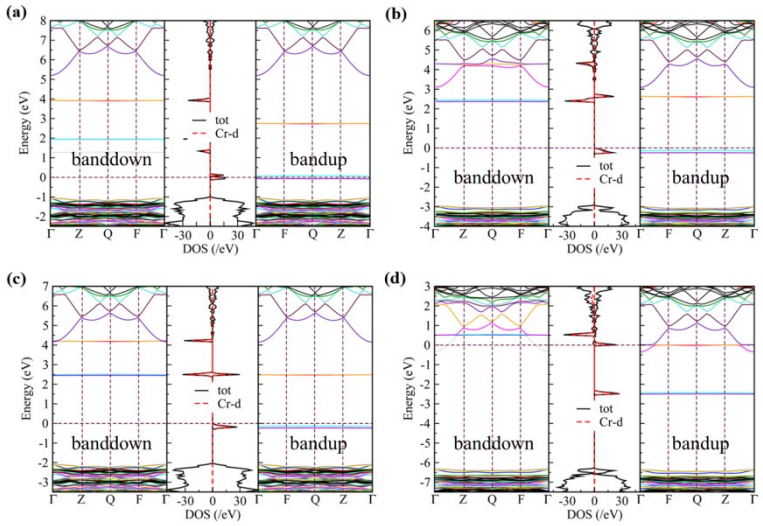

Figure S5 (colour online) The electronic structures of Al_2O_3:Cr in the calculations of OTL $\varepsilon_f(Cr^{n+/(n-1)+})$. (a) and (c) are the initial states with n = 4 and 3, while (b) and (d) are the final state with n = 4 and 3. The Fermi level is set to 0 eV.

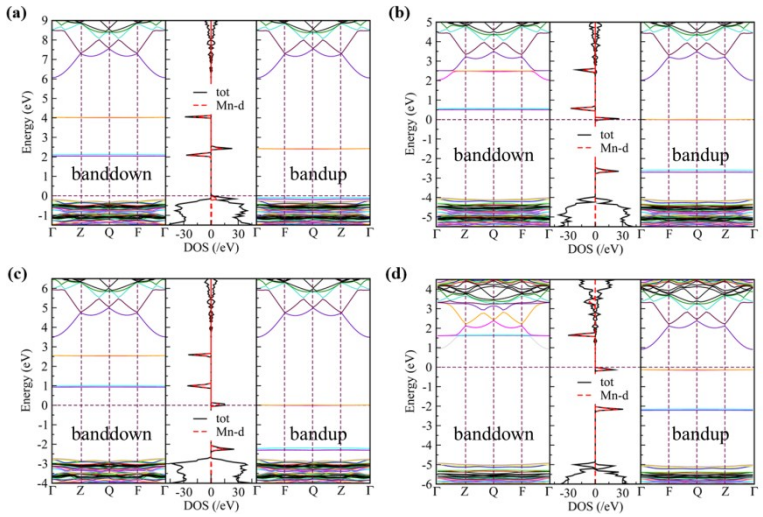

Figure S6 (colour online) The electronic structures of Al_2O_3:Mn in the calculations of OTL $\varepsilon_f(Mn^{n+/(n-1)+})$. (a) and (c) are the initial states with n = 4 and 3, while (b) and (d) are the final state with n = 4 and 3. The Fermi level is set to 0 eV.

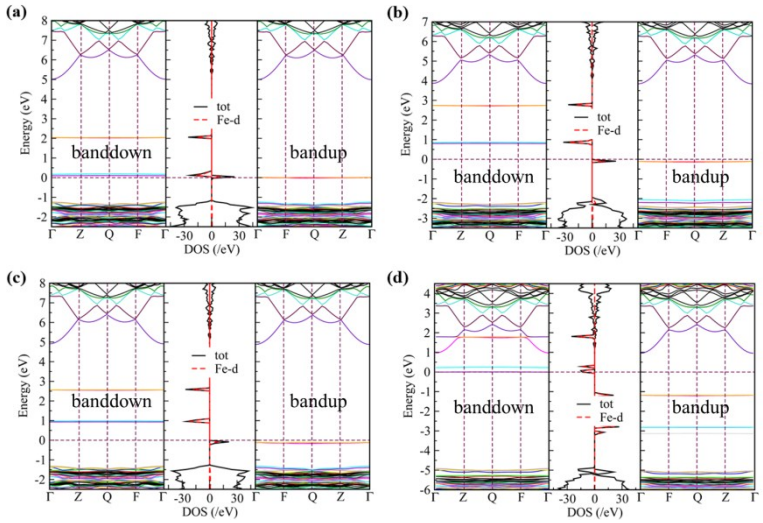

Figure S7 (colour online) The electronic structures of Al_2O_3:Fe in the calculations of OTL $\varepsilon_f(Fe^{n+/(n-1)+})$. (a) and (c) are the initial states with n = 4 and 3, while (b) and (d) are the final state with n = 4 and 3. The Fermi level is set to 0 eV.

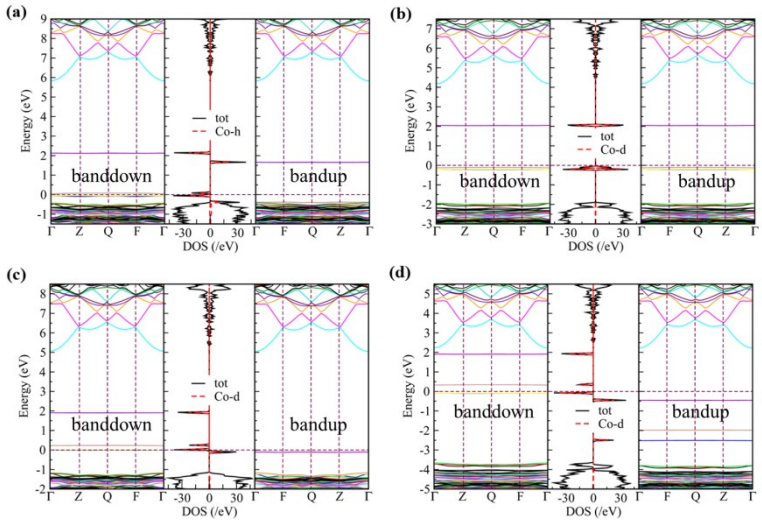

Figure S8 (colour online) The electronic structures of Al_2O_3:Co in the calculations of OTL $\varepsilon_f(Co^{n+/(n-1)+})$. (a) and (c) are the initial states with n = 4 and 3, while (b) and (d) are the final state with n = 4 and 3. The Fermi level is set to 0 eV.

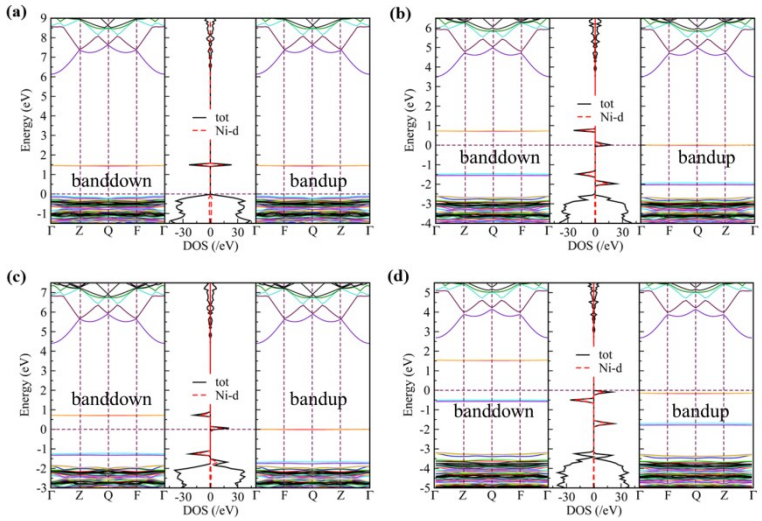

Figure S9 (colour online) The electronic structures of Al_2O_3:Ni in the calculations of OTL $\varepsilon_f(Ni^{n+/(n-1)+})$. (a) and (c) are the initial states with n = 4 and 3, while (b) and (d) are the final state with n = 4 and 3. The Fermi level is set to 0 eV.

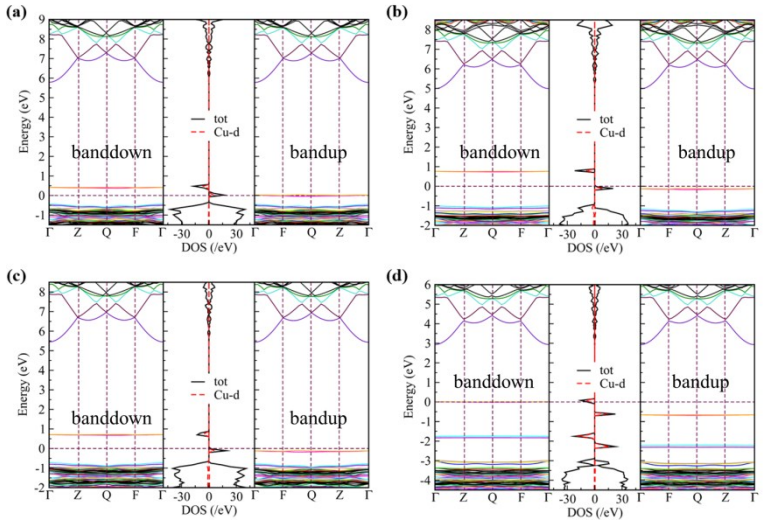

Figure S10 (colour online) The electronic structures of Al_2O_3:Cu in the calculations of OTL $\varepsilon_f(Cu^{n+/(n-1)+})$. (a) and (c) are the initial states with n = 4 and 3, while (b) and (d) are the final state with n = 4 and 3. The Fermi level is set to 0 eV.

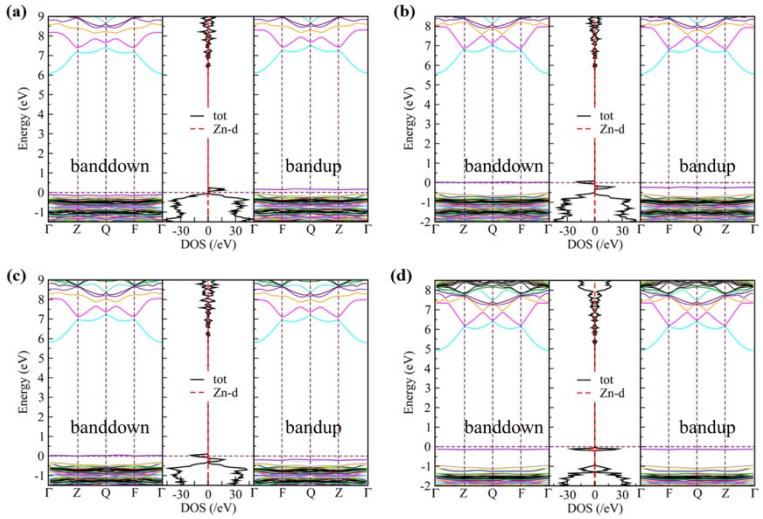

Figure S11 (colour online) The electronic structures of Al_2O_3:Zn in the calculations of OTL $\varepsilon_f(Zn^{n+/(n-1)+})$. (a) and (c) are the initial states with n = 4 and 3, while (b) and (d) are the final state with n = 4 and 3. The Fermi level is set to 0 eV.

C. The electronic structure of different valence states of X in $Y_3Al_5O_{12}$

In this part, only the 3d-TM ions doping in the octahedral site of $Y_3Al_5O_{12}$ have been considered. The resulting electronic structures are shown from Fig.S12 to Fig.S21. The 3d orbitals of Sc^{3+} are empty and locate in the conduction bands at the PBE level. So, when adding another electron to the system, this electron occupies the lower conduction

band rather than the 3d orbitals, as shown in Fig.S12. Thus, the resulting $\varepsilon_f(Sc^{3+/2+})$ is inaccurate. Similar case has also been found in the calculation of Ti^{2+} and Cr^{2+}. These results are distinguished in Fig.2 by hollow symbols. For the final states of $\varepsilon_f(Ti^{4+/3+})$ and $\varepsilon_f(V^{3+/2+})$, although a small part of the added electron occupies the lower conduction bands, most of the electron locates in the 3d states. So the errors in these situations should be smaller than those in $\varepsilon_f(Sc^{3+/2+})$ and we do not distinguish them from other results in Fig.2.

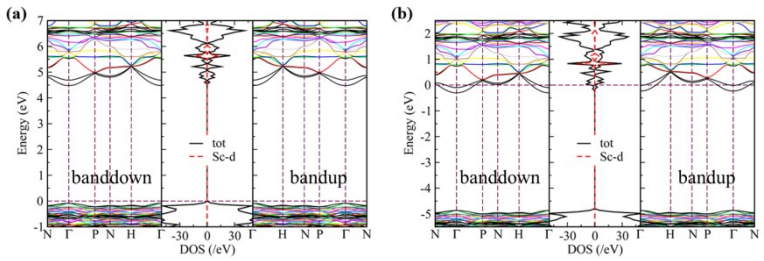

Figure S12 (colour online) The electronic structures of $Y_3Al_5O_{12}$:Sc in the calculations of OTL $\varepsilon_f(Sc^{n+/(n-1)+})$. (a) is the initial states with n = 3, and (b) is the final states with n = 3. The Fermi level is set to 0 eV.

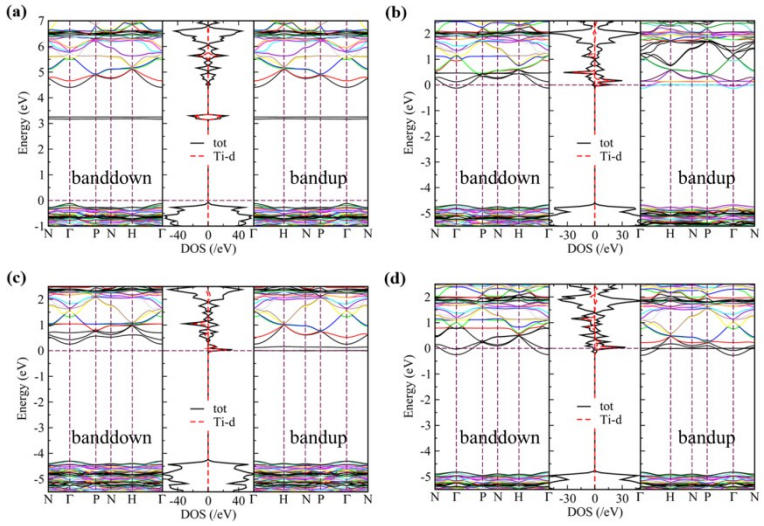

Figure S13 (colour online) The electronic structures of $Y_3Al_5O_{12}$:Ti in the calculations of OTL $\varepsilon_f(Ti^{n+/(n-1)+})$. (a) and (c) are the initial states with n = 4 and 3, while (b) and (d) are the final state with n = 4 and 3. The Fermi level is set to 0 eV.

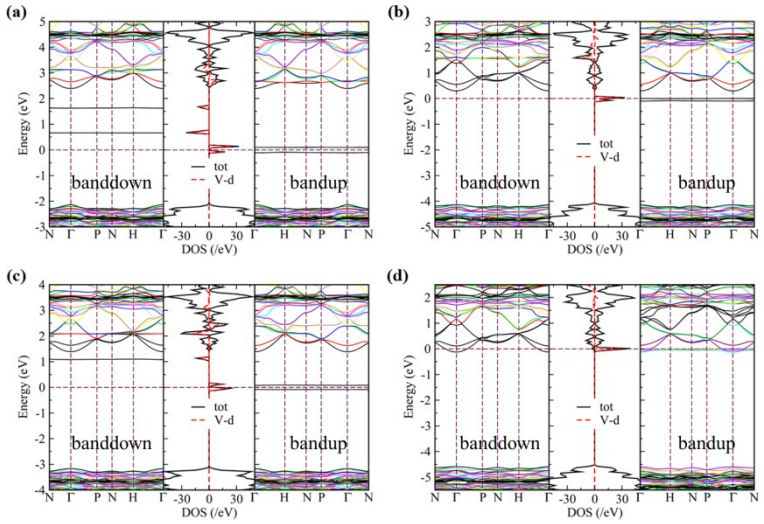

Figure S14 (colour online) The electronic structures of $Y_3Al_5O_{12}$:V in the calculations of OTL $\varepsilon_f(V^{n+/(n-1)+})$. (a) and (c) are the initial states with n = 4 and 3, while (b) and (d) are the final state with n = 4 and 3. The Fermi level is set to 0 eV.

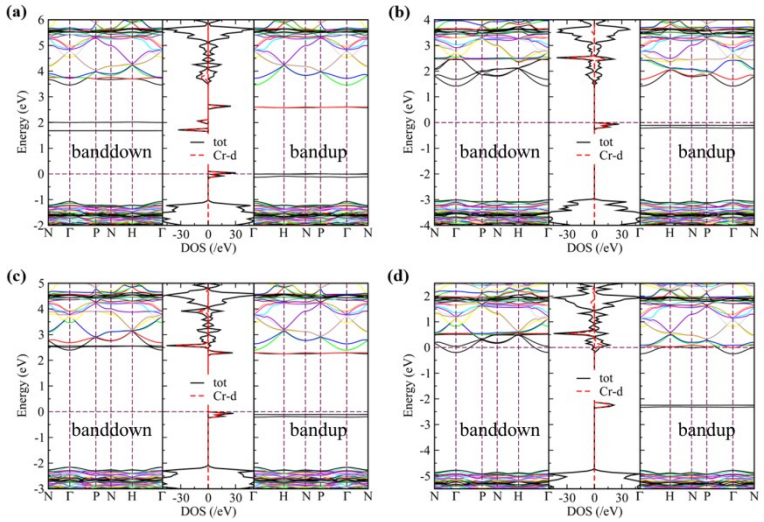

Figure S15 (colour online) The electronic structures of $Y_3Al_5O_{12}$:Cr in the calculations of OTL $\varepsilon_f(Cr^{n+/(n-1)+})$. (a) and (c) are the initial states with n = 4 and 3, while (b) and (d) are the final state with n = 4 and 3. The Fermi level is set to 0 eV.

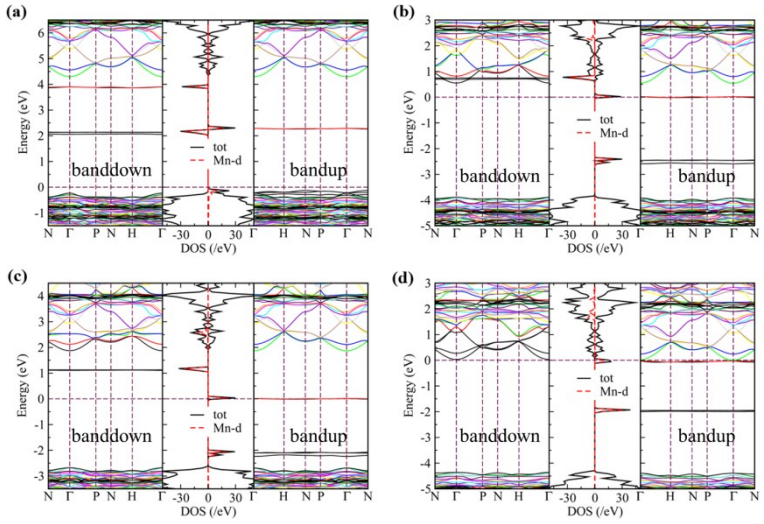

Figure S16 (colour online) The electronic structures of $Y_3Al_5O_{12}$:Mn in the calculations of OTL $\varepsilon_f(Mn^{n+/(n-1)+})$. (a) and (c) are the initial states with n = 4 and 3, while (b) and (d) are the final state with n = 4 and 3. The Fermi level is set to 0 eV.

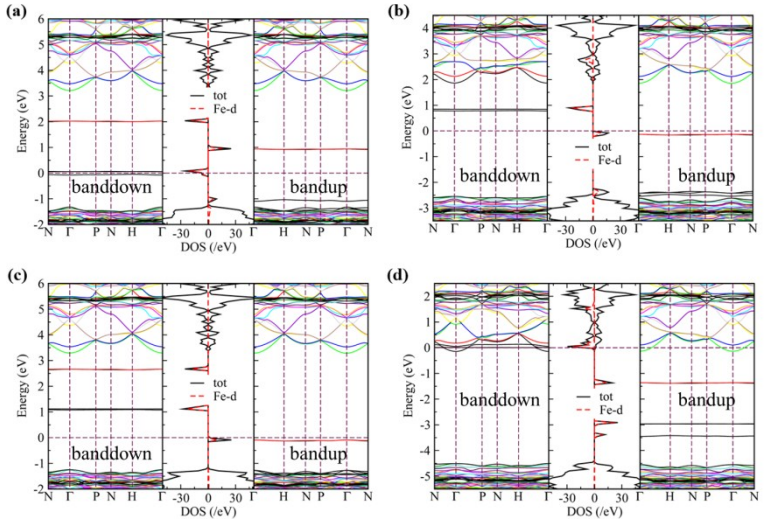

Figure S17 (colour online) The electronic structures of $Y_3Al_5O_{12}$:Fe in the calculations of OTL $\varepsilon_f(Fe^{n+/(n-1)+})$. (a) and (c) are the initial states with n = 4 and 3, while (b) and (d) are the final state with n = 4 and 3. The Fermi level is set to 0 eV.

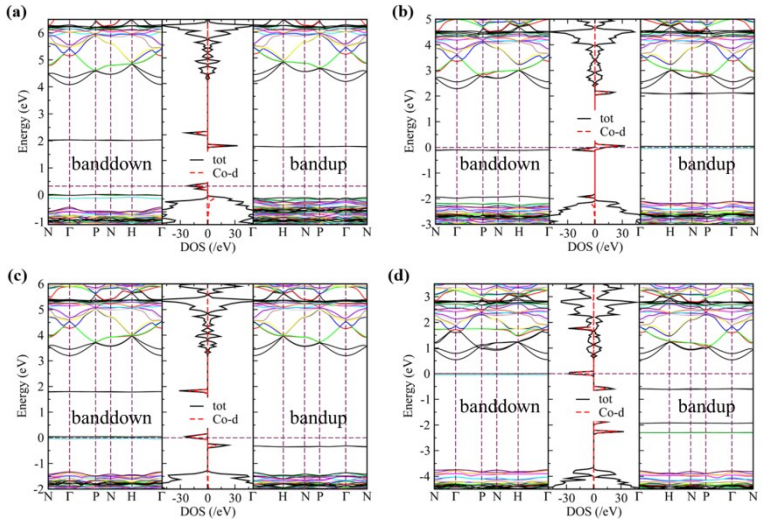

Figure S18 (colour online) The electronic structures of $Y_3Al_5O_{12}$:Co in the calculations of OTL $\varepsilon_f(Co^{n+/(n-1)+})$. (a) and (c) are the initial states with n = 4 and 3, while (b) and (d) are the final state with n = 4 and 3. The Fermi level is set to 0 eV.

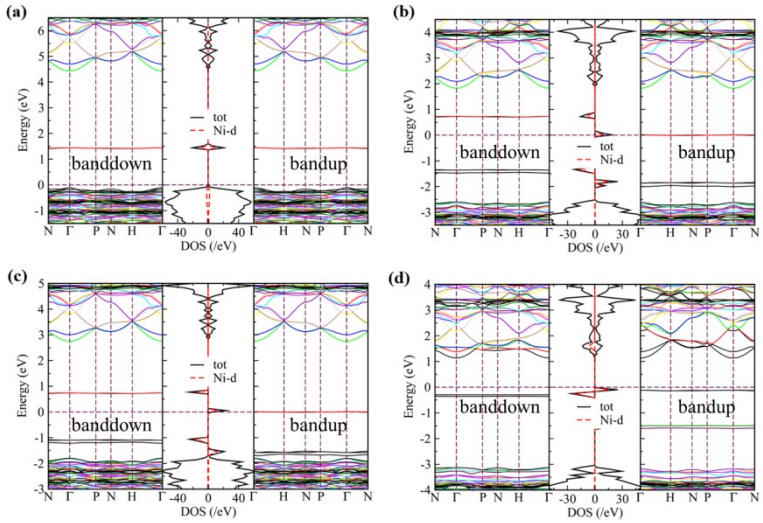

Figure S19 (colour online) The electronic structures of $Y_3Al_5O_{12}$:Ni in the calculations of OTL $\varepsilon_f(Ni^{n+/(n-1)+})$. (a) and (c) are the initial states with n = 4 and 3, while (b) and (d) are the final state with n = 4 and 3. The Fermi level is set to 0 eV.

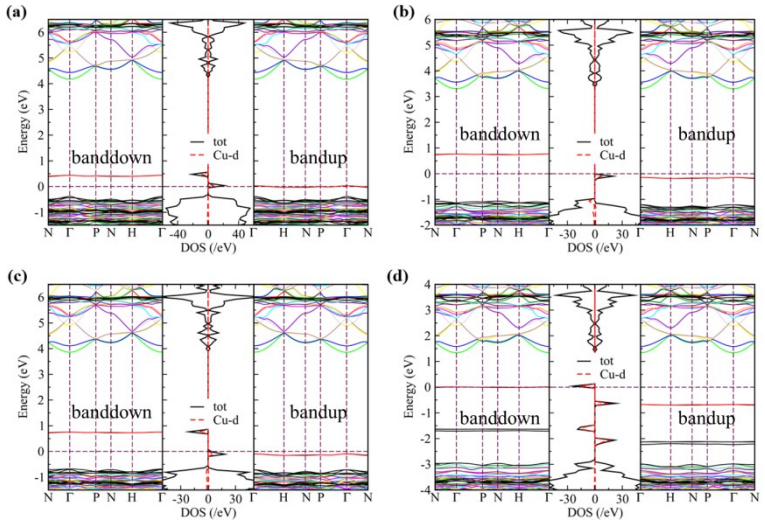

Figure S20 (colour online) The electronic structures of $Y_3Al_5O_{12}$:Cu in the calculations of OTL $\varepsilon_f(Cu^{n+/(n-1)+})$. (a) and (c) are the initial states with n = 4 and 3, while (b) and (d) are the final state with n = 4 and 3. The Fermi level is set to 0 eV.

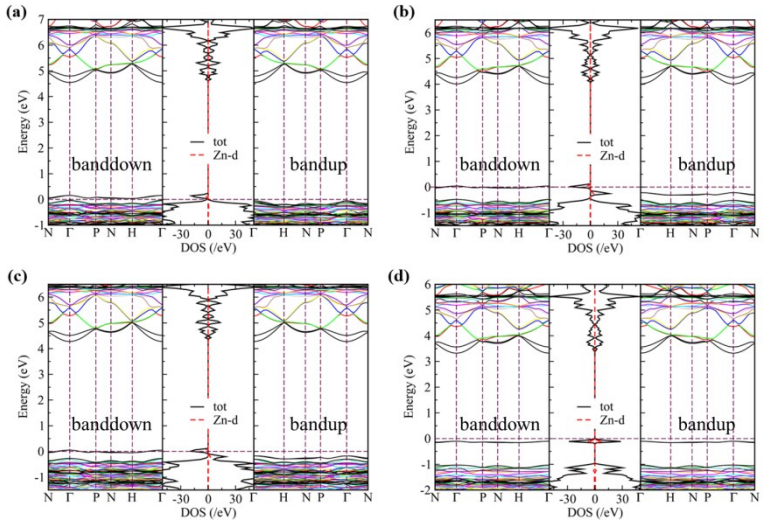

Figure S21 (colour online) The electronic structures of $Y_3Al_5O_{12}$:Zn in the calculations of OTL $\varepsilon_f(Zn^{n+/(n-1)+})$. (a) and (c) are the initial states with n = 4 and 3, while (b) and (d) are the final state with n = 4 and 3. The Fermi level is set to 0 eV.

D. Absorption spectra observed at room temperature for $GdAlO_3:Fe^{3+}$

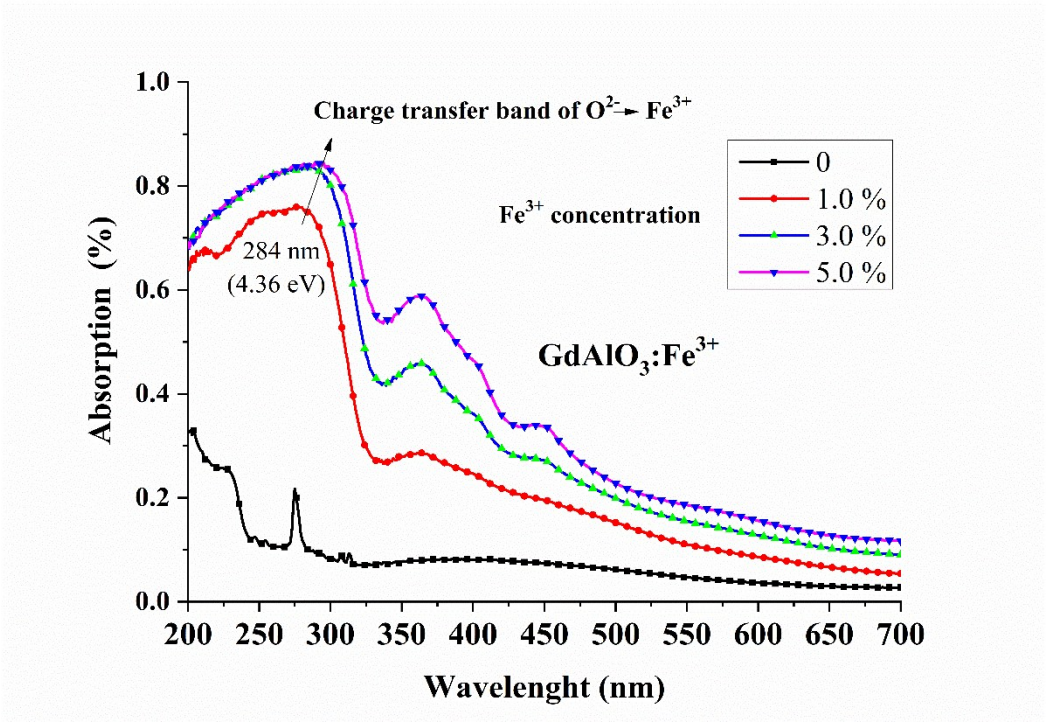

Figure S22 (colour online) The absorption spectra observed at room temperature for $^{Gd}\mathrm{Al}_{1-x}\mathrm{O}_3{:}^{Fe}{}^{3+}_{x}$. Their broad charge transfer band (CTB) can be observed from 255 to 298 nm. Here, the CTB maximum of $^{Gd}\mathrm{Al}_{0.99}\mathrm{O}_3{:}^{Fe}{}^{3+}_{0.01}$is estimated to be about 4.36 eV. We adopt this value to talk about the VRBE of $Fe^{3+/2+}$ in $GdAlO_3$.

1. P. Dorenbos, *Physical Review B*, 2013, **87**, 035118.
2. P. Dorenbos, *J. Lumin.*, 2013, **134**, 310-318.